Journal of Environmental Chemical Engineering 7 (2019) 102908

Contents lists available at ScienceDirect

Journal of Environmental Chemical Engineering

journal homepage: www.elsevier.com/locate/jece

Arsenate and arsenite removal from contaminated water by iron oxides nanoparticles formed inside a bacterial exopolysaccharide

Barbara Casentini[a,*], Michele Gallo[b], Franco Baldi[b]

[a] Water Research Institute, National Research Council of Italy (IRSA - CNR), Via Salaria, km 29.300, Monterotondo, Rome 00015, Italy
[b] Department of Molecular Sciences and Nanosystems, Cà Foscari University, Via Torino 155, 30172 Venice, Italy

ARTICLE INFO

Keywords:
Arsenic
Drinking water
Bioremediation
Exopolysaccharide
Iron nanoparticles

ABSTRACT

In the last decades, the presence of high As levels in groundwaters poses a serious limitation to the use of this resources for drinking purposes in several parts of the world. Treatment of As-rich waters selected iron oxides filters as more effective, low cost and selective technology. Green and biologically-driven pathways to synthetize new nanostructured iron oxy-hydroxides are becoming always more attractive. We tested the suitability of FeOOH nanoparticles (9–15 nm) produced by *Klebsiella oxytoca* strain DSM 29614 and encapsulated in EPS gel structure to treat arsenic rich water. Different gel:water volume ratios were tested to treat 5000 µg As/L solution. 20% FeEPS solution was able to remove 95% of As(V) while in 5% solution removal was reduced to 60%. Arsenic adsorption was very fast and follows pseudo-2nd order kinetic with maximum adsorption capacity reached at about 30 min. Adsorption followed Langmuir model for As(V) with q_{max} = 31.8 mg_{As}/g_{Fe} and BET for As(III) with 8 mg_{As}/g_{Fe} for the first layer in 10% FeEPS solution. FeEPS dried into powder showed noticeable removal only after 2 h, hence not suitable for drinking water treatment. Treatment of natural As levels in mimicked groundwaters showed 87–95% As(V) and 45–61% As(III) removal after 5 min. FeEPS gel immobilized onto bivalve shell debris was used in packed-bed filters. It retained 49.8 mg_{As}/g_{Fe} from 150 µg/L As(V) spiked groundwater before reaching breakthrough at 8000 BVs. Biologically produced FeEPS gel showed good potentialities as eco-friendly material to remove As from contaminated groundwater.

1. Introduction

Worldwide the presence of elevated natural arsenic concentration in aquifers in groundwater is often limiting its use as drinking water in several parts of the world. In Europe Directive 98/83/EC imposed the limit to 10 µg/L in waters intended for human consumption. Among arsenic removal technologies, adsorption processes gained the upper hand and granular iron hydroxides (GFH) filters are the most widely installed due to GFH natural availability, low cost and easy maintenance. even if its average adsorption capacity is not exceptional and in the range 5–10 $mg_{As}/g_{adsorbent}$ [1].

In the last decades the use of nanoparticles (NPs) in water treatment has been explored. Nano-sized adsorbents showed enhanced reactivity promoted by higher surface area leading to substantial increase in adsorption rates, if compared to granular or powdered adsorption materials. In addition the high efficiency of the nanomaterials reduces filter volume with smaller footprints, suitable for decentralized application and point-of-use-systems [2–4]. In particular nano-metallic oxides, i.e. iron oxy-hydroxides (FeOOH) nanoparticles, have been successfully tested for As removal [3]. Several nanostructured iron oxy-hydroxides (FeNPs) exhibited good As removal efficiency (10–120 $mg_{As}/g_{adsorbent}$) in aqueous systems: akaganeite [β-FeOOH] [5–7]; Zr-doped akaganeite [8]; maghemite [γ-Fe_2O_3] [9–11]; magnetite [Fe_3O_4] [12–14]; goethite [α-FeOOH] [15,16]; metal oxides heterostructures [17–22]. Chemical syntheses of iron NPs are commonly used, but they are often energy consuming and employ toxic chemicals. There is a growing need to develop reliable and eco-friendly experimental protocols for the synthesis of NPs [23,24]. The biological route is a viable solution, requiring in most of the cases ambient temperature, low pressure, neutral pH and generating uniform NPs with size ranging from 5 to 100 nm [25]. Saif et al. (2016) listed various green agents usable for the synthesis of iron NPs such as polymers, amino acids, bacteria, fungi, plant extracts, etc., and drafted their reaction pathways. Since 90′s, it was reported that dissimilatory Fe(III)-reducing microorganisms can couple the oxidation of organic materials to the reduction of Fe(III), giving as end-product ultrafine-grained magnetite [26]. Other bacteria were able to synthetize magnetite: *Desulfovibrio magneticus* strain RS^{-1}, *Thermoanaerobacter ethanolicus*, *Magnetospirillum magnetotacticum*,

* Corresponding author.
E-mail address: casentini@irsa.cnr.it (B. Casentini).

https://doi.org/10.1016/j.jece.2019.102908
Received 26 November 2018; Received in revised form 8 January 2019; Accepted 13 January 2019
Available online 22 January 2019

Shewanella putrefaciens strain $GS^{-1}5$ [23]. Bacterial fermentation represents a fundamental new approach for large-scale production of nanometer-sized crystalline particles. [27] reported that under anaerobic laboratory conditions, *Klebsiella oxytoca* strain DSM 29,614 (ex $BAS^{-1}0$) fermented Fe(III)-citrate and Na-citrate giving CH_3COOH and CO_2 with a simultaneous production of a considerable amount of ferric hydrogel, composed by branched heptasaccharide repeating units exopolysaccharide (EPS) with metal content up to 36 wt% [28,29]. The production of FeEPS under anaerobic conditions is a strategy adopted by the strain to survive in extreme conditions such as acid mine drainages with high heavy metal concentrations. This strategy could be efficiently used to produce large amount of valuable FeEPS, starting from a low cost substrate as Fe(III) citrate. Furthermore, FeNPs encapsulated in EPS have the advantage that gel structure functions as capping agent preventing clustering and flocculation of NPs.

It is known that negative charges/complexing molecules present in the EPS are able to interact with potentially toxic metals (Cd, Cu, Pb, Ni, Hg…) positively charged. Removal process follows several possible pathways [30]: the creation of electrostatic bonds among metals and negatively charged groups (i.e. carboxylic and phosphoric groups), ion exchange with protons present on the surface and the formation of a metal–ligand coordination bond [31]. In most cases, the ionic nature of metal, its size and charge density in turn regulates its interaction with negatively charged EPS [30]. On the contrary, literature on the removal of negatively charged oxyanions (i.e. arsenate, chromate, selenite, vanadate …) is rare. The presence of iron oxy-hydroxides NPs in EPS may extend the bioremediation use of this material to anionic classes of contaminants.

The application of FeEPS to sequester arsenic species sounds very promising. Therefore, we tested the potentialities of *green* FeOOH-EPS to treat As-rich drinking water. FeEPS NPs were tested in the form of hydrogel and dehydrated powder to evaluate best performance for a successful drinking water treatment. Different aspects were elucidated, i.e. the form of the biosorbent more effective (hydrogel vs powder), kinetic aspects of the removal process and related adsorption isotherms at different concentrations of As(III), As(V) and matrices. Adsorption processes were evaluated through batch studies by the application of kinetic and isotherm adsorption models. A preliminary column (*packed bed*) study was also carried out to test efficiency to remove As of FeEPS adsorbed onto a solid support.

2. Experimental

2.1. Reagents

All chemicals and reagents were of analytical grade. Arsenic (V) and (III) stock solutions (1000 mg/L) were prepared using Na_2HAsO_4*$7H_2O$ (Fluka) and Na_2AsO_2 (Fluka), respectively. Iron (III) and (II) stock solutions (1000 mg/L) were prepared from $Fe(NO_3)_3$*9H2O (Merck) and $FeSO_4$*$7H_2O$ (Sigma Aldrich), respectively. HNO_3 (Merck, Suprapur), HCl (Merck, Suprapur), sodium acetate (Riedel-Hahn), acetic acid (Carlo Erba), *Ortho*-phenantroline (Sigma Aldrich), hydroxylamine (Sigma Aldrich) were used for the FeEPS digestion and Fe detection.

2.2. Production of biogenerated FeEPS

Iron NPs hydrogel (FeEPS) was synthetized by *Klebsiella oxytoca* strain DSM 29,614 isolated from acid mine drainage. Details Fe(III) citrate fermentation process and EPS structure could be found elsewhere [28]. At stationary phase, the strain produces a ferric exopolymeric hydrogel with entrapped Fe NPs [32], similar to ferric hydroxides in ferritin [33]. FeEPS was extracted by the bacterial culture and precipitated using 70% ethanol solution at 4 °C. In our experiments alcoholic fraction was removed by washing with MilliQ water. Fe NPs embedded in the EPS gel were 9–15 nm [32,33] with +2.82 average Fe valence [33]. FeEPS powder was produced by drying the gel in oven at 30 °C. After acid digestion (Section 2.3), measured Fe content of FeEPS gel and powder was 2.5 ± 0.2 mg_{Fe}/ml and 0.3 ± 0.1 mg_{Fe}/mg_{powd}, respectively.

2.3. Analytical methods

Temperature, pH and conductivity (EC) were in situ measured by probes (Hach HQ 30 d). Total arsenic was measured by Atomic Absorption Spectrometry (Perkin Elmer AAnalyst 800) equipped with Ir-coated THGA furnace. Spectrophotometric Fe determination required hydroxylamine pre-reduction and *O*-phenantroline complexation with present Fe^{+2} at acetate buffered conditions (pH = 4.5). Red complexes were read at 512 nm [34]. Fe content in stock Fe-EPS gel and Fe-EPS powder was measured by digesting 20 ml of Fe-EPS with 2 ml HNO_3 or 50 mg Fe-EPS powder with 4.5 ml HCl + 2 ml HNO_3. Total Fe solubilisation was achieved by heating at 40 °C for 30 min and Fe spectrophotometrically quantified after dilution. Z-potential measurements were carried out using 1 ml 10% FeEPS solution in the pH range 2.5–7 by Zetasizer Nano (Lavern Instruments). Point of zero charge (pH_{pzc}) was calculated from the plot (Annex A1).

2.4. Experimental setup

Batch and column studies were carried out in MilliQ water at controlled pH and on real matrices using two different groundwaters of Medium conductivity (M_EC, 500 μS/cm) and High conductivity (H_EC, 1000 μS/cm), rich in sulphate and carbonate (Annex A2).

2.4.1. Adsorption kinetic batch tests

A preliminary kinetic test was run to evaluate potential As removal by different FeEPS ratio (v:v) and Fe concentration in solution after 5 min 9000 rpm (10,414 rcf) centrifugation and/or 0.2 μm filtration (acetate cellulose). FeEPS gel solutions were prepared by adding 2 ml FeEPS stock solution to different MilliQ volumes in the range 1:1 up to 1:250 (ml_{FeEPS} :ml_{water}). Solutions were spiked 1000 μg/L As(V) and analysed after 10 min to calculate As removal. Preliminary test evidenced the good potential of FeEPS gel to fast remove As but excessive concentration of Fe in surnatant solution was found after centrifugation and 0.2 μm sample filtration was then always required. Arsenic removal after 10 min ranged from 4.8 to 94.3% (Annex A3). Considering to avoid high density of the Fe rich gel (not suitable for drinking water) and the removal efficiency, 1:5 (20% FeEPS, Gel 1) and 1:20 (5% FeEPS, Gel 2) dilutions were chosen to run first kinetic tests. 1:10 (10% FeEPS) was chosen to perform further kinetic, adsorption, desorption and column tests. Arsenic removal by Gel 1 and 2 was studied in 250 ml batches spiked 5000 μg/L As(V) at pH 7 ± 0.5and sampled at selected time intervals (1; 5; 10; 30; 60; 120 and 360 min). During a second test, the performances of gel and powder FeEPS were compared in 50 ml solution at pH 7 ± 0.5 with lower As initial concentration [2000 μg/L As(V)]. Fe gel and powder solutions were prepared at two different dilutions: 20% (Gel 3, Powder 1) and 5% (Gel 4, Powder 2) by keeping similar Fe amount between powder and gel. Solutions were sampled at 0.2, 0.5, 1, 2, 3.5, 6 and 24 h. A summary of all kinetic tests conditions is given in Table 1.

In MilliQ and real matrices (M_EC and H_EC) similar to As-rich groundwaters exploited for human consumption in Italy at an 150 μg/L initial As(V) or As(III), arsenic removal efficiency was tested using 10% FeEPS (5 ml in 50 ml, 11.3 mg Fe) in fast kinetic study (35 min) [35,36]. Samples were collected at 5, 10, 20 and 35 min. To evaluate the adsorption properties of 10% FeEPS gel under consecutive As exposures, batch adsorption was repeated by discarding surnatant and adding again new 50 ml As solution at 150 μ/L As-rich water to same FeEPS gel. After the third consecutive adsorption, 50 ml MilliQ water were added to centrifuged FeEPS in order to test possible desorption processes of trapped As from FeEPS. Samples were taken after 16 h and 3 days.

Table 1
Summary of kinetic tests carried out using different hydrogel solutions and dried FeEPS powder.

	Gel 1	Gel 2	Gel 3	Gel 4	Powder 1	Powder 2
Fe amount (mg)	**135**	**34**	**24.2**	**6**	**25.6**	**6.4**
[Fe] (mg Fe/L)	*540*	*108*	*484*	*120*	*512*	*128*
Volume *(mL)*	*250*	*250*	*50*	*50*	*50*	*50*
% FeEPS	20%	5%	20%	5%	Equivalent to 20%	Equivalent to 5%
time (min)	**As Removal (%)**					
10	**86%**	**44%**	**23%**	**5%**	**0%**	**0%**
360	**95%**	**59%**	**27%**	**20%**	**33%**	**21%**
1440			35%	33%	59%	44%
$[AsV]_0$ *($\mu g_{As}/L$)*	*5000*	*5000*	*2000*	*2000*	*2000*	*2000*
Initial As:Fe *(mg_{As}/g_{Fe})*	*9.3*	*36.8*	*4.1*	*16.7*	*3.9*	*15.6*
q_{360} *(mg_{As}/g_{Fe})*	***8.8***	***21.5***	***1.1***	***3.4***	***1.3***	***3.3***

2.4.2. Adsorption batch isotherms

Maximum adsorption capacity (q_{max}) was calculated for both As(III) and As(V) in 10% FeEPS (4.8 mg Fe in 20 ml, 240 mg_{Fe}/L) and 20% FeEPS powder (10.4 mg_{Fe} in 20 ml, 520 mg_{Fe}/L) in batch studies. Initial As concentration ranged from 0.25 to 20 mg/L and pH was 7 ± 0.5. Samples were collected after 20 h.

2.4.3. Column study

Small column (Ø 1 cm, H 8 cm) fed by H_EC water at 10 ml/min was initially prepared using FeEPS hydrogel, but after few minutes clogging occurred. A new material was then prepared by dispersing FeEPS hydrogel onto crushed carbonaceous natural material (FeEPS solid). The latter is constituted by beached shells of *Cardium* spp, with a specific grain-size (1–3 mm) and low specific surface area of about 3 m^2/g. The total Fe content of this new mixed material was 0.01 $mg_{Fe}/mg_{adsorbent}$. Small column was filled with 4 g FeEPS solid (H 4 cm, Bed Volume 3.1 ml). Column was fed by H_EC spiked groundwater at 200 µg As(V)/L and flow set to 10 ml/min (0.6 L/h, linear velocity 7.6 m/h, EBCT 18.8 s).

2.5. Adsorption models

Several kinetics and thermodynamics models to describe arsenic adsorption processes have been previously reported [37–41].

2.5.1. Kinetic models

The use of kinetic equations helps to better identify mechanisms of adsorption, identification of rate-determining steps and predict the adsorption rate. Generally, liquid/solid adsorption involves three main processes: film diffusion, intraparticle diffusion and mass action. In physical adsorption, mass action is very fast, therefore the rate limiting steps usually correspond with the other two processes [42].

2.5.1.1. Pseudo 1st and 2nd order kinetic models. Data obtained by batch experiments were analysed by employing linearized *pseudo*-first order (1) and *pseudo*-second order (2) equations:

$$q_t = q_1[1 - e^{-k_1 t}] \text{pseudo 1st order} \quad (1)$$

$$q_t = q_2 \frac{k_2 q_2 t}{1 + k_2 q_2 t} \text{pseudo 2nd order} \quad (2)$$

where q_t is the amount of As adsorbed (mg/g) at time *t*, q_1 is *pseudo* 1st order maximum adsorption capacity (mg/g) and q_2 for the pseudo 2nd order equation, k_1 is the *pseudo*-first order rate constant (min^{-1}) and k_2 is the *pseudo*–second order rate constant (g/mg min) [43]. Usually the pseudo-first order equation apply to reversible adsorption reactions while the pseudo-second order kinetic model consider chemical adsorption as the rate determining step. Parameters were calculated using SOLVER tool in Excel by minimizing Sum of Squares according to the abovementioned kinetic equations in non-linearized form.

2.5.1.2. Weber-Morris. In order to test if intraparticle diffusion, usually the rate-limiting step in arsenic adsorption, was involved and limiting the adsorption process, Weber and Morris (1963) diffusion model was applied to our data:

$$q_t = k_{int} t^{1/2} + C_i \quad (3)$$

where q_t (mg/g) is the amount of As adsorbed at time t at equilibrium, k_{int} (mg/g $min^{1/2}$) is the rate parameter of the intra-particle diffusion control stage and C_i (mg/g) indicates the thickness of the boundary layer. This model suggests that if adsorption mechanism is via intraparticle diffusion then the plot will be linear when is the sole rate-limiting step it will pass through the origin [41,42]. When the sorption process is controlled by more than one mechanism, then the plot will be multilinear and a multistage processes could be identified [41,44].

2.5.2. Adsorption isotherm models

Among the several available models usually used to fit adsorption experiments, we selected Langmuir, Freundlich and BET isotherm models [45].

2.5.2.1. Langmuir isotherm. This model describes solute-adsorbent equilibrium by assuming a monolayer coverage with all sites energetically equally probable [46]. It follows the equation:

$$q_e = \frac{q_{max} b C_e}{1 + b C_e} \quad (1)$$

where q_e is the measured equilibrium adsorption capacity (mg_{As}/g_{Fe}), C_e is the measured equilibrium solute concentration (mg/L), q_{max} is the maximum adsorption capacity of a monolayer stratum (mg_{As}/g_{Fe}) and *b* is the coefficient of Langmuir bond energy (L/mg) given by adsorption/desorption constants ratio.

2.5.2.2. Freundlich isotherm. This empirical model considers adsorption sites at different energies with stronger binding sites firstly occupied [46]. It follows the equation:

$$q_e = K_f C_e^{1/n} \quad (2)$$

where q_e is the measured equilibrium adsorption capacity (mg_{As}/g_{Fe}), C_e is the measured equilibrium solute concentration (mg/L), K_f is an indicator of the adsorption capacity (L/mg) increasing simultaneously with the increase of maximum adsorption capacity and *1/n* is an indicator of adsorption intensity.

2.5.2.3. BET isotherm. Originally developed to describe gas/solid adsorption, its application has been extended also to describe multi-layers adsorption processes. BET isotherm represents an extension of Langmuir model, and it hypothesizes that further adsorption is possible on the first adsorption layer even when first strata adsorption sites coverage is not completed yet [47]. It follows the equation:

$$q_e = \frac{K_b C_e q_{max}}{(C_s - C_e)[1 + (K_b - 1)\frac{C_e}{C_s}]} \quad (3)$$

where q_e is the measured equilibrium adsorption capacity (mg_{As}/g_{Fe}), C_e is the measured equilibrium solute concentration (mg/L), C_S is solute concentration saturating first layer (mg/L), q_{max} is the maximum adsorption capacity of a monolayer stratum (mg_{As}/g_{Fe}) corresponding to Langmuir model. If $C_s >> C_e$ and $K_b >> 1$, BET isotherm follows Langmuir. Due the difficulties in value parameters determination, it has been suggested to suppose at a first stage a plausible value for C_S and iteratively calculate all the parameters to approach R^2 as close as possible to 1.

2.5.3. Models evaluation

The goodness of fit was then evaluated by calculating the coefficient of determination (R^2) and the Root Mean Square Error (RMSE), where R^2 represents the relative measure of fit (*trend prediction*), while RMSE is an absolute measure of fit (*model accuracy*).

$$\text{Coefficient of Determination } \mathbf{R}^2 = \frac{\sum (\mathbf{x_m} - \overline{\mathbf{x_e}})^2}{\sum (\mathbf{x_m} - \overline{\mathbf{x_e}})^2 + \sum (\mathbf{x_m} - \mathbf{x_e})^2} \quad (4)$$

$$\text{Root Mean Square Error } \boldsymbol{RMSE} = \sqrt{\frac{1}{\boldsymbol{n}} \sum_{i=1}^{i=n} (\boldsymbol{x_m} - \boldsymbol{x_e})^2} \quad (5)$$

where x_m is the value given by the model, x_e is the experimental data and $\bar{x}_e$ is the mean value of experimental dataset [48].

3. Results and Discussion

3.1. Kinetic behaviour of FeEPS

Arsenate adsorption at initial concentration of 5000 µg/L was 95.1% and 58.6% for 20% FeEPS (135 mg Fe) and 5% FeEPS (34 mg Fe), respectively (Fig. 1). Within first 30 min was already 90.1% for 20% FeEPS and 41.8% for 5% FeEPS.

Even if 5% FeEPS solution was less effective in terms of total removal, its final adsorption capacity was higher, being 21.5 mg_{As}/g_{Fe} instead of 8.8 mg_{As}/g_{Fe} at higher FeEPS concentration. FeEPS gel showed pH_{pzc} of 3.2 (Annex A1), hence at working pH of 7 exhibits a negative surface charge not favouring oxyanions adsorption. Usually pH_{pzc} for FeOOH mineral phases is around 6.5–9.5 [49] and at natural pH their positive charge is promoting adsorption of negatively charged arsenate. By applying kinetic models (Section 2.5.1), we concluded that adsorption follows pseudo-2nd order kinetic for both FeEPS dilutions with $R^2 = 0.75$ and RMSE = 0.43 for 20% FeEPS and $R^2 = 0.59$ and RMSE = 2.67 for 5% FeEPS (See Annex A4). Higher adsorption in concentrated gel could be explained by higher amount of adsorption sites in solution, but at this gel concentration, repulsion forces could also reduce specific adsorption. In this case the limiting step should be represented by the penetration of the so-called "boundary layer". Weber-Morris intraparticle diffusion model was applied (Fig. 1) in order to elucidate which processes were involved during As adsorption in FeEPS hydrogel and their influence on the overall adsorption. Weber-Morris plot evidenced as in both cases the straight line did not pass through zero hence the presence of a boundary layer, but no multistage process is observed and the only limiting-rate process was intraparticle diffusion, before reaching an equilibrium plateau. The thickness of boundary layer given by the intercept correspond to 6.5 and 11.1 mg/g for 20% and 5% FeEPS. Contrary to what observed by other authors [39,41], the lack of an initial stage related to film diffusion suggested that boundary layer was not limiting in our case. We finally hypothesize that at the same time EPS may exert repulsion with As ions but also facilitate the entrapment into the gel by EPS polysaccharides driven chelation and speeding up the adsorption process, as evidenced by higher adsorption rate during first minutes, in line with what evidenced for positively charged potentially toxic metals [30]. The high chelation efficiency of EPS has recently been confirmed for Hg^{2+} [50].

Due to the difficulties that may occur while managing gel formulation in drinking water treatment, kinetic tests were also carried out on dried FeEPS powder. Hydrogel *vs* powder, containing similar Fe concentrations (mg/L), were tested at initial 2000 µg/L As(V) for 24 h at two adsorbent:solution ratios (see Table 1 for details). FeEPS powder adsorption showed slow removal increasing only after 2 h up to 24 h (Fig. 2), most probably caused by reduced penetrability of this dried material and less accessibility for As to adsorption sites. In hydrogel As desorption was observed after 2 h and after one day removal stabilized to a value around 35% for both Gel 3 and Gel 4. On a long-term basis, powder formulation may be also effective, since removal reached 59% in Powder 1 and 44% in Powder 2.

Even during these experiments, despite the lower content of Fe (≈ 35 mg at 20% FeEPS and 6 mg at 5% FeEPS), diluted solutions showed highest adsorption capacity: 3.4 versus 1.1 mg_{As}/g_{Fe} in gel and 3.3 *versus* 1.1 for powder. Lower adsorption capacity, if compared first kinetic results, were due to lower initial As:Fe ratio (see Table 1).

At last fast kinetic experiment was carried out in different real water matrices at varying ionic contents (see Section 2.4.1 and Annex A2) and natural occurring groundwater concentration for both species As(V) and As(III). After 10 min in real groundwaters, FeEPS formed naked-eye visible clusters and coagulated due to salting-out effect. Arsenate removal was 87–95% after only 5 min and increased a little further up to 30 min (Fig. 3). Best removal capacity was observed in M_EC groundwater (up to 97%) with As concentration always below drinking water limit (10 µg/L, European Directive 98/83/EC). Arsenite removal was initially fast as well but less performing with 45–61% As(III) removed after 5 min and a significant increase after 30 min. Best final removal (74%) was again obtained in M_EC water, followed by MilliQ (69%) and H_EC water (62%).

In line with what observed by [51], the presence of sulfate did not influence much arsenate adsorption but resulted in a considerable reduction in arsenite adsorption. At circumneutral pH, better As(V) adsorption respect to uncharged As(III) is due to its negative charge that can quickly react with $-OH_2^+$ group onto Fe oxy-hydroxides surface [52]. Best efficiency of M−EC water, could be attributed to a better buffer capacity to pH 7–7.5 than MQ, which limited the natural pH increase following arsenate adsorption. While on the other side higher ionic strength water (H−EC) reduced As(V) ions mobility towards charged adsorption sites. Furthermore, [53] carried out a specific study of arsenate adsorption onto hematite and highlighted the possible influence of carbonate on enhancing As(V) uptake. Effect of dissolved carbonate on As(V) adsorption depends on several conditions [e.g., surface available sites, initial As(V) and reaction times] and under certain conditions carbonate become competing ion to As(V).

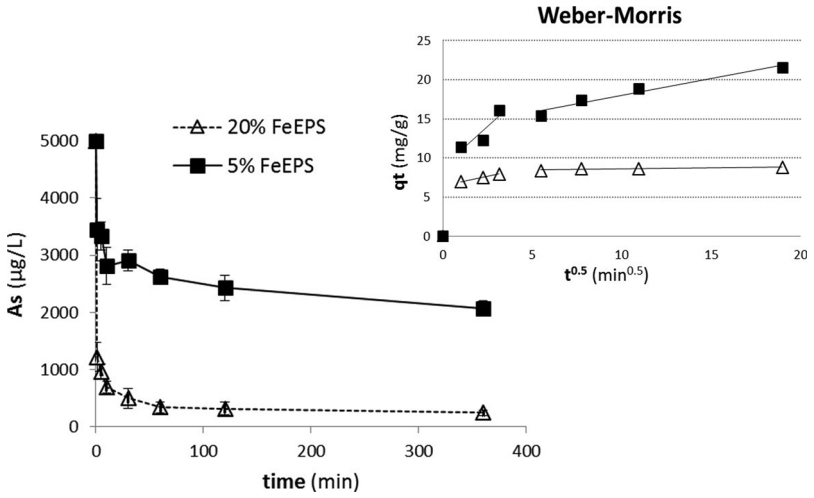

Fig. 1. Arsenate adsorption kinetic at different gel dilution (5% and 20% FeEPS) and As(V) = 5000 µg/L. Related intraparticle diffusion model (Weber-Morris) trends are also reported.

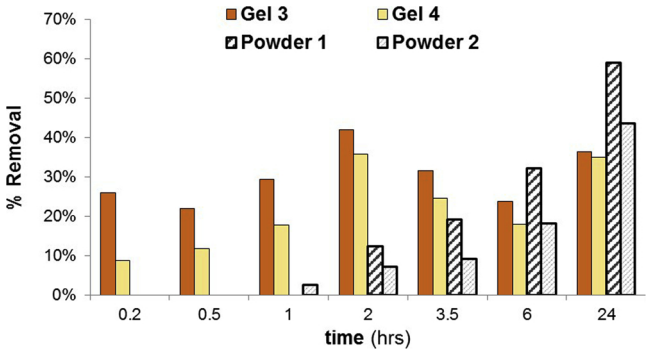

Fig. 2. Comparison of As adsorption using FeEPS in gel and powder (more details in Annex A4).

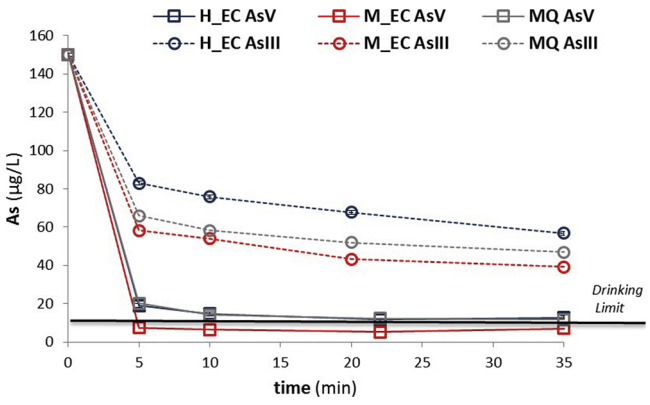

Fig. 3. Fast adsorption in real matrices at different ionic strengths at 150 µg/L initial As concentration. Drinking water limit at 10 µg/L is reported as straight black line.

3.2. Adsorption and desorption processes

Isotherm adsorption tests were carried out in the range 0.25–20 mg/L using 10% FeEPS for both As(V) and As(III) and 5% FeEPS powder only for As(V). Elaborated isotherms showed very different shapes with higher adsorption for As(V) (Fig. 4). On the contrary, higher initial As concentrations increased arsenite adsorption due to facilitated intraparticle diffusion of this neutral specie within the mesoporous FeEPS structure.

Isotherm models summary is reported in Table 2 and fits in Annex A5. Langmuir isotherm best fit As(V) adsorption in both gel and powder. Equilibrium maximum adsorption capacity (q_{max}) was 31.8 mg_{As}/g_{Fe}, for FeEPS gel while 26.8 mg_{As}/g_{Fe} for FeEPS powder. Arsenite adsorption showed a typical multilayer adsorption, as confirmed by best fit of BET model to this dataset, with 1st layer adsorption capacity of 8.0 mg_{As}/g_{Fe}. FeEPS adsorption capacities replicate average iron oxy-hydroxide capacity of 20–60 mg_{As}/g_{Fe} usually reported in literature [1,41,54].

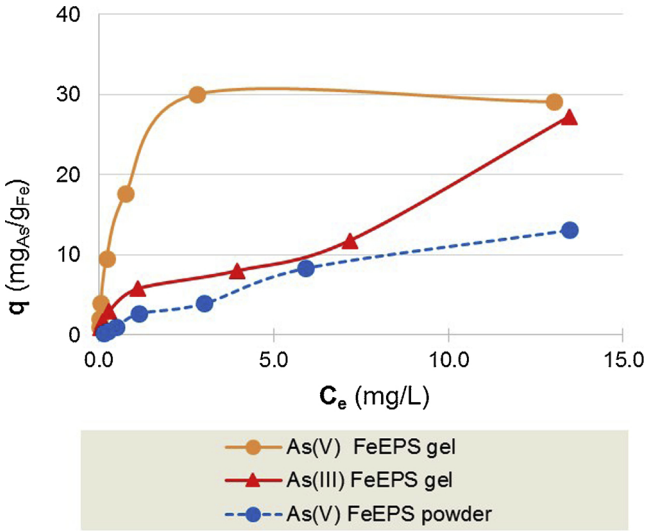

Fig. 4. Arsenic adsorption isotherms as function of As speciation and adsorbent material Adsorption isotherm on powder showed lower As(V) removal capacity compared to hydrogel.

Adsorption capacity of 10% FeEPS gel after consecutive exposures to 150 µg/L of both As(V) and As(III) was tested after 30 min contact time (see Section 2.4.1). After 1st adsorption As(V) removal was above 90% and As(III) above 50% in all water matrices. After 3rd adsorption run, arsenate removal decreased to 56–66% and arsenite to 25–37%. The amount of As adsorbed after all three consecutive adsorption was 1.45–1.61 mg_{As}/g_{Fe} for As(V) and 0.78–1.08 mg_{As}/g_{Fe} for As(II) with in both cases higher amount for M_EC water (see Table 3). If we consider that Fe milliequivalents in solution were 3 order of magnitude higher than those of As, the observed adsorption capacity decrease of FeEPS gel, about 30–40 % for both species and in all matrices, could not be attributed to lack of adsorption sites but to As species reduced access. This aspect should be carefully evaluated for FeEPS gel application and

Table 2
Isotherms models applied to As(V) and (III) removal in both gel and powder FeEPS material. Parameters characteristics of each model are reported together with R^2 and RMSE to evaluate the goodness of model fit.

		As(V) gel	As(III) gel	As(V) powder	
Freundlich $q_e = K_f * C_e^{(1/n)}$	K_f (L/mg)	16.85	4.40	2.14	
	n	3.76	1.70	1.42	
	R^2	0.8573	0.8986	0.9869	
	RMSE	4.0	2.9	0.5	
Langmuir $q_e = q_{max} b C_e/(1+bC_e)$	b (L/mg)	2.07	0.81	0.07	
	q_{max} (mg_{As}/g_{Fe})	31.8	12.4	26.8	
	R^2	**0.9796**	0.9399	**0.9900**	
	RMSE	**1.5**	0.9	**0.4**	
	C_s (mg/L)	33146	19.0	29.5	
BET $q_e = K_b C_e q_{max}/(C_s-C_e)[1+(K_b-1)C_e/C_s]$	K_b	68634	32.5	10.5	
	q_{max} (mg_{As}/g_{Fe})	31.8	8.0	8.0	
	R^2	0.9795	**0.9964**	0.9826	
	RMSE	1.5	**0.5**	0.6	

Table 3
Columns with reddish headings report removal efficiencies in 3 water matrices for both As(V) and As(III) in the case of consecutive adsorptions. In blueish headings, columns refer to % of As desorbed after 16 hs and 3 days contact time with MilliQ. Grey cells refer to As(V) and white cells to As(III). Arsenic desorption was calculated according to following expression: [As released in solution (mg)]/[Cumulative amount of As adsorbed ($Ads_1 + Ads_2 + Ads_3$) in mg].

	Ads_1	Ads_2	Ads_3	TOT Ads mg_{As}/g_{Fe}	Des 16 hrs	Des 3 days
MQ **AsV**	92%	67%	60%	**1.45**	12%	7%
MQ **AsIII**	69%	43%	37%	**0.99**	5%	1%
M_EC **AsV**	95%	82%	66%	**1.61**	4%	2%
M_EC **AsIII**	74%	53%	35%	**1.07**	9%	3%
H_EC **AsV**	92%	76%	56%	**1.49**	7%	6%
H_EC **AsIII**	55%	38%	25%	**0.78**	12%	4%

potentialities. Low pH_{pzc} of FeEPS, unfavourable for oxyanions adsorption, and the possible simultaneous role of complexing molecules present in the EPS gel, could promote desorption phenomena when As-free solution is in contact with the adsorbent. Desorption test showed low As release in solution, corresponding to 5–12% after 16 hs and 1–7 % after 3 days, with no large differences among As(V) and As(III) and evidences of re-equilibration of adsorption in the long run.

3.3. FeEPS efficiency under continuous removal

A preliminary column study was carried out to evaluate FeEPS efficiency once immobilized on a solid support (bivalve shell debris) and under continuous regime. A small column containing only 4 g of adsorbent (40 mg Fe) was fed at 10 ml/min. Before reaching complete breakthrough (C_0/C_i close to 1), column treated about 25 L of H-EC water, corresponding to approximately 8000 BVs. Arsenic removal quickly decreased to 50% (Fig. 5) and outflow As concentration was always above the drinking limit of 10 µg/L, but this was expected due to the reduced dimension of the used packed-bed. On the other side, the final amount of As adsorbed onto Fe present was 49.8 mg_{As}/g_{Fe}, indicating good performance of the FeEPS solid material that it could

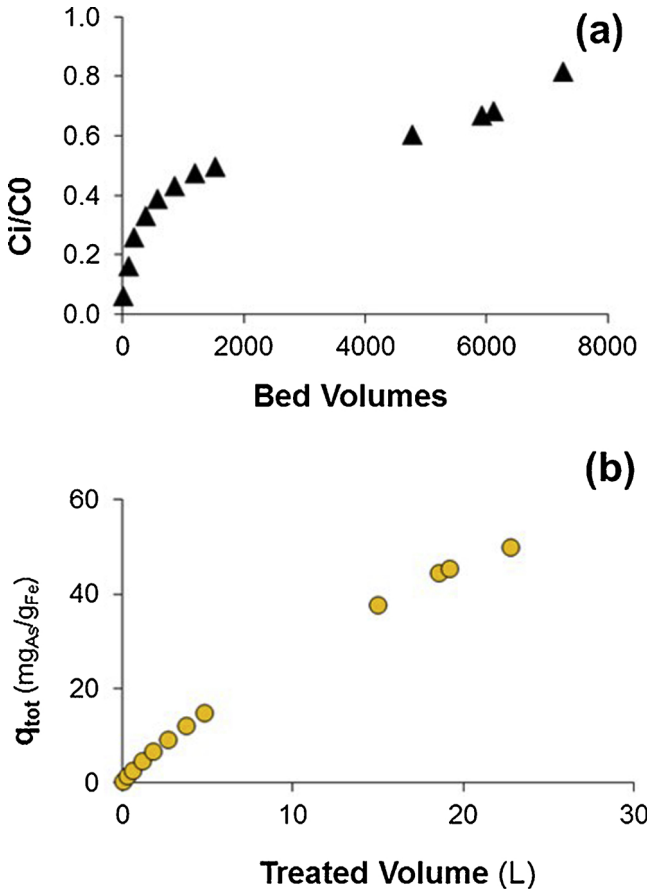

Fig. 5. Arsenic removal capacity in packed-bed fed by 200 µg/L As(V) spiked groundwater (H-EC) at 10 ml/min.

surely represent a promising way of using Fe biogenerated NPs in adsorption filters. Iron in the outflow was always absent, indicating lack of FeEPS detachment from support. Long-term pilot scale studies based on larger volume filters are advisable to understand the real potentialities of this material to treat As-rich groundwater for the production on drinking water.

4. Conclusions

The growing interest in water treatment to find environmentally safe technologies for water and soil remediation motivates interest towards biologically based technological approaches. Recently biosorption through microbial biomass and their products is one of the most studied [30]. At the same time the amazing efficiency of NPs also valued nano-sized materials application in this sector, especially Fe oxy-hydroxides [55]. The implementation of advanced nanotechnology to traditional water and wastewater technology processes treatments offers new opportunities in these fields [3]. The combination of bacterial-driven synthesis with nanotechnology, it is now widely explored due to the reduced environmental impact of new biogenerated materials, elevated efficiency and their reduced costs. For instance, commercially nano-sized magnetite (25–50 nm) may cost $500/kg while microbial processes are potentially capable of producing 5–90 nm pure or substituted magnetites at a fraction of the cost of traditional chemical synthesis (Moon et al., 2010). In the last decades, arsenic nano- and bioremediation has received significant attention due to its cost effectiveness and environmental compatibility [56–58].

Our results showed that biologically produced FeEPS gel has good potentialities as “green” material to remove As from contaminated waters (drinking and waste waters) with possible application for soil remediation, as well. Fast kinetic, good adsorption capacity (both as hydrogel or deposited onto solid) and efficiency in real groundwater render this material suitable for As-rich groundwater treatment. Processes involved in the adsorption and the specific role of Fe NPs and EPS matrix in As removal should be further investigated. EPS could be improved by functionalization/doping it to reduce negative surface charges. A protocol to improve its adsorption/embedding into porous solid structure is also required to implement the use of this materials for the removal of oxyanions (As, Cr, V, Se) removal in a continuous fixed bed reactor on a long term basis.

Main findings were:

- FeEPS hydrogel have pH_{pzc} corresponding to 3.2, hence less favourable to arsenic adsorption than Fe oxy-hydroxides nanoparticles;
- Arsenic adsorption was very fast and follows pseudo-2nd order kinetic with maximum adsorption capacity reached at about 30 min. Higher removal efficiency were recorded for more concentrated FeEPS solution due to higher amount of Fe-nanoparticles present, but specific adsorption capacity increased with solution dilution. Intraparticle diffusion within the pores appears the only involved and rate-limiting process suggesting that ionic repulsion could be balanced by other processes, i.e. chelation by EPS, that favours fast film diffusion. Treatment of natural As levels in mimicked groundwaters showed 87–95% As(V) and 45–61% As(III) removal after 5 min;
- Dehydrated FeEPS gel showed around 50% As removal on a long run but it is not suitable for drinking water application due to the extremely slow adsorption kinetics;
- Adsorption followed Langmuir process for As(V) and BET model with increased adsorption at higher initial As concentration for As (III). In FeEPS 10% solution q_{max} was 31.8 mg_{As}/g_{Fe} for As(V) while first layer As(III) adsorption was 8 mg_{As}/g_{Fe} with a 30% adsorption reduction after three consecutive adsorption for both As species;
- Desorption was below 10% hence As re-mobilization was limited;
- Immobilization of FeEPS onto carbonaceous shells was successful to obtain good filtering material able to adsorb 49.8 mg_{As}/g_{Fe} at initial As(V) concentration of 150 µg/L before reaching breakthrough at 8000 BVs.

Acknowledgement

Authors acknowledge the financial support by Italian MIUR PRIN 2010-2011 project (Grant agreement No 2010JBNLJ7-002).

Appendix A. Supplementary data

Supplementary material related to this article can be found, in the online version, at doi:https://doi.org/10.1016/j.jece.2019.102908.

References

[1] D. Mohan, C.U. Pittman, Arsenic removal from water/wastewater using adsorbents-a critical review, J. Hazard. Mater. 142 (2007) 1–53, https://doi.org/10.1016/j.jhazmat.2007.01.006.
[2] S. Bhattacharya, I. Saha, A. Mukhopadhyay, D. Chattopadhyay, U. Chand, ISSN 2249-8532 Original Article Role of nanotechnology in water treatment and purification: potential applications and implications, 3 (2013) 59–64.
[3] I. Gehrke, A. Geiser, A. Somborn-Schulz, Innovations in nanotechnology for water treatment, Nanotechnol. Sci. Appl. 8 (2015) 1–17, https://doi.org/10.2147/NSA.S43773.
[4] P. Westerhoff, P. Alvarez, Q. Li, J. Gardea-Torresdey, J. Zimmerman, Overcoming implementation barriers for nanotechnology in drinking water treatment, Environ. Sci. Nano 3 (2016) 1241–1253, https://doi.org/10.1039/C6EN00183A.
[5] E. Deliyanni, D.N. Bakoyannakis, I. Zouboulis, K. Matis, Sorption of As (V) ions by akaganeite-type nanocrystals, 50 (2003) 155–163.
[6] E. Deliyanni, L. Nalbandian, K. Matis, Adsorptive removal of arsenites by a nanocrystalline hybrid surfactant-akaganeite sorbent, J. Colloid Interface Sci. 302 (2006) 458–466, https://doi.org/10.1016/j.jcis.2006.07.007.
[7] Y.X. Zhang, Y. Jia, A facile solution approach for the synthesis of akaganéite (β-FeOOH) nanorods and their ion-exchange mechanism toward As(V) ions, Appl. Surf. Sci. 290 (2014) 102–106, https://doi.org/10.1016/j.apsusc.2013.11.007.
[8] X. Sun, C. Hu, X. Hu, J. Qu, M. Yang, Characterization and adsorption performance of Zr-doped akaganéite for efficient arsenic removal, J. Chem. Technol. Biotechnol. 88 (2013) 629–635, https://doi.org/10.1002/jctb.3878.
[9] T. Tuutijärvi, J. Lu, M. Sillanpää, G. Chen, As(V) adsorption on maghemite nanoparticles, J. Hazard. Mater. 166 (2009) 1415–1420, https://doi.org/10.1016/j.jhazmat.2008.12.069.
[10] S.R. Chowdhury, E.K. Yanful, A.R. Pratt, Arsenic removal from aqueous solutions by mixed magnetite-maghemite nanoparticles, Environ. Earth Sci. 64 (2011) 411–423, https://doi.org/10.1007/s12665-010-0865-z.
[11] M. Auffan, J. Rose, O. Proux, D. Borschneck, A. Masion, P. Chaurand, J.L. Hazemann, C. Chaneac, J.P. Jolivet, M.R. Wiesner, A. Van Geen, J.Y. Bottero, Enhanced adsorption of arsenic onto maghemites nanoparticles: As(III) as a probe of the surface structure and heterogeneity, Langmuir. 24 (2008) 3215–3222, https://doi.org/10.1021/la702998x.
[12] J.T. Mayo, C. Yavuz, S. Yean, L. Cong, H. Shipley, W. Yu, J. Falkner, A. Kan, M. Tomson, V.L. Colvin, The effect of nanocrystalline magnetite size on arsenic removal, Sci. Technol. Adv. Mater. 8 (2007) 71–75, https://doi.org/10.1016/j.stam.2006.10.005.
[13] Z. Bujňáková, P. Baláž, A. Zorkovská, M.J. Sayagués, J. Kováč, M. Timko, Arsenic sorption by nanocrystalline magnetite: an example of environmentally promising interface with geosphere, J. Hazard. Mater. 262 (2013) 1204–1212, https://doi.org/10.1016/j.jhazmat.2013.03.007.
[14] C.T. Yavuz, J.T. Mayo, C. Suchecki, J. Wang, A.Z. Ellsworth, H. D'Couto, E. Quevedo, A. Prakash, L. Gonzalez, C. Nguyen, C. Kelty, V.L. Colvin, Pollution magnet: nano-magnetite for arsenic removal from drinking water, Environ. Geochem. Health 32 (2010) 327–334, https://doi.org/10.1007/s10653-010-9293-y.
[15] M.K. Ghosh, G.E.J. Poinern, T.B. Issa, P. Singh, Arsenic adsorption on goethite nanoparticles produced through hydrazine sulfate assisted synthesis method, Korean J. Chem. Eng. 29 (2012) 95–102, https://doi.org/10.1007/s11814-011-0137-y.
[16] D.N. Bakoyannakis, E. Deliyanni, I. Zouboulis, K. Matis, L. Nalbandian, T. Kehagias, Akaganeite and goethite-type nanocrystals: synthesis and characterization, Microporous Mesoporous Mater. 59 (2003) 35–42, https://doi.org/10.1016/S1387-1811(03)00274-9.
[17] K. Gupta, T. Basu, U.C. Ghosh, Sorption characteristics of arsenic (V) for removal from water using agglomerated nanostructure Iron (III) -Zirconium (IV) bimetal mixed oxide, Engineering (2009) 2222–2228.
[18] K. Gupta, K. Biswas, U.C. Ghosh, Nanostructure Iron (III) - zirconium (IV) binary mixed oxide : synthesis, characterization, and physicochemical aspects of arsenic (III) sorption from the Aqueous Solution, Ind. Eng. Chem. Res. (2008) 9903–9912, https://doi.org/10.1021/ie8002107.
[19] K. Gupta, U.C. Ghosh, Arsenic removal using hydrous nanostructure iron(III)-titanium(IV) binary mixed oxide from aqueous solution, J. Hazard. Mater. 161 (2009) 884–892, https://doi.org/10.1016/j.jhazmat.2008.04.034.

[20] L. Chen, H. Xin, Y. Fang, C. Zhang, F. Zhang, X. Cao, X. Li, Application of metal oxide heterostructures in arsenic removal from contaminated water, J. Nanomater. (2014) 1–10 http://www.hindawi.com/journals/jnm/2014/793610/.
[21] Z. Ren, G. Zhang, J. Paul Chen, Adsorptive removal of arsenic from water by an iron-zirconium binary oxide adsorbent, J. Colloid Interface Sci. 358 (2011) 230–237, https://doi.org/10.1016/j.jcis.2011.01.013.
[22] Y.M. Zheng, S.F. Lim, J.P. Chen, Preparation and characterization of zirconium-based magnetic sorbent for arsenate removal, J. Colloid Interface Sci. 338 (2009) 22–29, https://doi.org/10.1016/j.jcis.2009.06.021.
[23] S. Iravani, Bacteria in Nanoparticle Synthesis: Current Status and Future Prospects, Int. Sch. Res. Not. 2014 (2014) 1–18, https://doi.org/10.1155/2014/359316.
[24] S. Saif, A. Tahir, Y. Chen, Green synthesis of Iron nanoparticles and their environmental applications and implications, Nanomaterials 6 (2016) 209, https://doi.org/10.3390/nano6110209.
[25] K.Revati Abhilash, B.D. Pandey, Microbial synthesis of iron-based nanomaterials—a review, Bull. Mater. Sci. 34 (2011) 191–198, https://doi.org/10.1007/s12034-011-0076-6.
[26] D.R. Lovley, Magnetite formation during microbial dissimilatory iron reduction, Iron Biominer. Springer US, Boston, MA, 1991, pp. 151–166, https://doi.org/10.1007/978-1-4615-3810-3_11.
[27] F. Baldi, A. Minacci, M. Pepi, A. Scozzafava, Gel sequestration of heavy metals by Klebsiella oxytoca isolated from iron mat, FEMS Microbiol. Ecol. 36 (2001) 169–174 (accessed March 1, 2017), http://www.ncbi.nlm.nih.gov/pubmed/11451521.
[28] S. Leone, C. De Castro, M. Parrilli, F. Baldi, R. Lanzetta, Structure of the iron-binding exopolysaccharide produced anaerobically by the gram-negative BacteriumKlebsiella oxytoca BAS-10, Eur. J. Org. Chem. 2007 (2007) 5183–5189, https://doi.org/10.1002/ejoc.200700302.
[29] F. Baldi, D. Marchetto, D. Battistel, S. Daniele, C. Faleri, C. De Castro, R. Lanzetta, Iron-binding characterization and polysaccharide production by Klebsiella oxytoca strain isolated from mine acid drainage, J. Appl. Microbiol. 107 (2009) 1241–1250, https://doi.org/10.1111/j.1365-2672.2009.04302.x.
[30] P. Gupta, B. Diwan, Bacterial Exopolysaccharide mediated heavy metal removal: a Review on biosynthesis, mechanism and remediation strategies, Biotechnol. Rep. Amst. (Amst) 13 (2017) 58–71, https://doi.org/10.1016/J.BTRE.2016.12.006.
[31] S. Comte, G. Guibaud, M. Baudu, Biosorption properties of extracellular polymeric substances (EPS) towards Cd, Cu and Pb for different pH values, J. Hazard. Mater. 151 (2008) 185–193, https://doi.org/10.1016/J.JHAZMAT.2007.05.070.
[32] F. Baldi, D. Marchetto, D. Zanchettin, E. Sartorato, S. Paganelli, O. Piccolo, A bio-generated Fe(III)-binding exopolysaccharide used as new catalyst for phenol hydroxylation, Green Chem. 12 (2010) 1405, https://doi.org/10.1039/c004967k.
[33] I. Arčon, O. Piccolo, S. Paganelli, F. Baldi, XAS analysis of a nanostructured iron polysaccharide produced anaerobically by a strain of Klebsiella oxytoca, BioMetals 25 (2012) 875–881, https://doi.org/10.1007/s10534-012-9554-6.
[34] B. Casentini, F.T. Falcione, S. Amalfitano, S. Fazi, S. Rossetti, Arsenic removal by discontinuous ZVI two steps system for drinking water production at household scale, Water Res. 106 (2016) 135–145, https://doi.org/10.1016/j.watres.2016.09.057.
[35] S. Fazi, S. Crognale, B. Casentini, S. Amalfitano, F. Lotti, S. Rossetti, The arsenite oxidation potential of native microbial communities from arsenic-rich freshwaters, Microb. Ecol. 72 (2016), https://doi.org/10.1007/s00248-016-0768-y.
[36] M. Rotiroti, E. Sacchi, L. Fumagalli, T. Bonomi, Origin of arsenic in groundwater from the multilayer aquifer in Cremona (Northern Italy), Environ. Sci. Technol. 48 (2014) 5395–5403, https://doi.org/10.1021/es405805v.
[37] Y.S. Ho, G. McKay, A comparison of chemisorption kinetic models applied to pollutant removal on various sorbents, Process Saf. Environ. Prot. 76 (1998) 332–340, https://doi.org/10.1205/095758298529696.
[38] Y.S. Ho, Review of second-order models for adsorption systems, J. Hazard. Mater. 136 (2006) 681–689, https://doi.org/10.1016/j.jhazmat.2005.12.043.
[39] Z.Ö. Kocabaş, Y. Yürüm, Kinetic modeling of arsenic removal from water by ferric ion loaded red mud, Sep. Sci. Technol. 46 (2011) 2380–2390, https://doi.org/10.1080/01496395.2011.595757.
[40] Y.N. Chen, L.Y. Chai, Y. De Shu, Study of arsenic(V) adsorption on bone char from aqueous solution, J. Hazard. Mater. 160 (2008) 168–172, https://doi.org/10.1016/j.jhazmat.2008.02.120.
[41] M.C.S. Faria, R.S. Rosemberg, Ca. Bomfeti, D.S. Monteiro, F. Barbosa, L.C. a Oliveira, M. Rodriguez, M.C. Pereira, J.L. Rodrigues, Arsenic removal from contaminated water by ultrafine δ-FeOOH adsorbents, Chem. Eng. J. 237 (2014) 47–54, https://doi.org/10.1016/j.cej.2013.10.006.
[42] H. Qiu, L. Lv, B. Pan, Q.Q. Zhang, W. Zhang, Q.Q. Zhang, Critical review in adsorption kinetic models, J. Zhejiang Univ. Sci. A. 10 (2009) 716–724, https://doi.org/10.1631/jzus.A0820524.
[43] J.-P. Simonin, On the comparison of pseudo-first order and pseudo-second order rate laws in the modeling of adsorption kinetics, Chem. Eng. J. 300 (2016) 254–263, https://doi.org/10.1016/J.CEJ.2016.04.079.
[44] B.I. Olu-Owolabi, P.N. Diagboya, K.O. Adebowale, Evaluation of pyrene sorption-desorption on tropical soils, J. Environ. Manage. 137 (2014) 1–9, https://doi.org/10.1016/j.jenvman.2014.01.048.
[45] K.Y. Foo, B.H. Hameed, Insights into the modeling of adsorption isotherm systems, Chem. Eng. J. 156 (2010) 2–10, https://doi.org/10.1016/j.cej.2009.09.013.
[46] G. Limousin, J.-P. Gaudet, L. Charlet, S. Szenknect, V. Barthès, M. Krimissa, Sorption isotherms: a review on physical bases, modeling and measurement, Appl. Geochem. 22 (2007) 249–275, https://doi.org/10.1016/J.APGEOCHEM.2006.09.010.
[47] S. Brunauer, P.H. Emmett, E. Teller, Adsorption of gases in multimolecular layers, J. Am. Chem. Soc. 60 (1938) 309–319, https://doi.org/10.1021/ja01269a023.
[48] J.-P. Simonin, On the comparison of pseudo-first order and pseudo-second order rate laws in the modeling of adsorption kinetics, Chem. Eng. J. 300 (2016) 254–263, https://doi.org/10.1016/J.CEJ.2016.04.079.
[49] R.M. Cornell, U. Schwertmann, The Iron Oxides: Structure, Properties, Reactions, Occurrences and Uses, 2nd ed., (2003) Weinheim.
[50] F. Baldi, M. Gallo, S. Daniele, D. Battistel, C. Faleri, A. Kodre, I. Arčon, An extracellular polymeric substance quickly chelates mercury(II) with N-heterocyclic groups, Chemosphere 176 (2017) 296–304, https://doi.org/10.1016/j.chemosphere.2017.02.093.
[51] A. Jain, R.H. Loeppert, Effect of competing anions on the adsorption of arsenate and arsenite by ferrihydrite, J. Environ. Qual. 29 (2000) 1422, https://doi.org/10.2134/jeq2000.00472425002900050008x.
[52] S. Dixit, J. Hering, Comparison of arsenic (V) and arsenic (III) sorption onto iron oxide minerals: implications for arsenic mobility, Environ. Sci. Technol. 37 (2003) 4182–4189, https://doi.org/10.1021/es030309t.
[53] Y. Arai, D.L. Sparks, J. Davis, Effects of dissolved carbonate on arsenate adsorption and surface speciation at the hematite-water interface, Environ. Sci. Technol. 38 (2004) 817–824, https://doi.org/10.1021/es034800w.
[54] W. Chen, R. Parette, J. Zou, F.S. Cannon, B.A. Dempsey, Arsenic removal by iron-modified activated carbon, Water Res. 41 (2007) 1851–1858, https://doi.org/10.1016/J.WATRES.2007.01.052.
[55] M. Mohapatra, S. Anand, Synthesis and applications of nano-structured iron oxides/hydroxides – a review, Int. Res. J. Eng. Sci. Technol. Innov. 2 (2011) 127–146, https://doi.org/10.4314/ijest.v2i8.63846.
[56] S. Fazi, S. Amalfitano, B. Casentini, D. Davolos, B. Pietrangeli, S. Crognale, F. Lotti, S. Rossetti, Arsenic removal from naturally contaminated waters: a review of methods combining chemical and biological treatments, Rend. Lincei. 27 (2016), https://doi.org/10.1007/s12210-015-0461-y.
[57] M.M. Bahar, M. Megharaj, R. Naidu, Bioremediation of arsenic-contaminated water: recent advances and future prospects, Water Air Soil Pollut. 224 (2013) 1722, https://doi.org/10.1007/s11270-013-1722-y.
[58] S. Lata, S.R. Samadder, Removal of arsenic from water using nano adsorbents and challenges: A review, J. Environ. Manage. 166 (2016) 387–406, https://doi.org/10.1016/j.jenvman.2015.10.039.